16th World Congress in Computational Mechanics (WCCM)
21-26 July 2024, Vancouver, Canada
A. Korobenko, M. Laforest, S. Prudhomme, R. Vaziri (Eds)

A KINEMATICALLY-EXACT REDUCED-ORDER ROD MODEL FOR ELASTOPLASTIC FAILURE IN THIN-WALLED STRUCTURES

MARCOS P. KASSAB[1], EDUARDO M. B. CAMPELLO[2] AND ADNAN IBRAHIMBEGOVIC[3]

[1] Polytechnic School of the University of São Paulo
P.O. Box 61548, 05424-970, São Paulo, SP, Brazil
marcos.kassab@usp.br, https://orcid.org/0000-0002-9543-1406

[2] Polytechnic School of the University of São Paulo
P.O. Box 61548, 05424-970 São Paulo, SP, Brazil
campello@usp.br and https://orcid.org/0000-0002-6770-9634

[3] Université de Technologie de Compiegne
Rue de docteur Schweitzer, 60200, Compiègne, Hauts-de-France, France
adnan.ibrahimbegovic@utc.fr, http://orcid.org/0000-0002-6502-0198

Key words: thin-walled beams, hardening, model reduction, multiscale modeling

Abstract. This work profits from a weakly coupled multiscale approach to derive a 7-DOF kinematically-exact reduced-order rod model for thin-walled members (starting from [1]) with a plastic hardening constitutive equation (based on [2]-[3]) that emulates the coupling between local buckling effects and hardening plasticity at material level. The model is implemented in an in-house finite element program for flexible thin structures and shall be validated against reference solutions. The novelty as compared to [2]-[3] is the extension to the fully 3D context, including torsion-warping degrees-of-freedom and arbitrary (plastic) failure mode capabilities, allowing for the modelling of complex structural problems involving thin-walled rod members. Although kinematically-exact rod models are able to detect critical loads and represent post-critical configurations in many common scenarios, issues are bound to emerge when local effects (such as buckling of web and/or flanges) are relevant, especially when they are coupled with plastic deformations. For rod models, the combination of those factors can be satisfactorily represented in a phenomenological way by embedding them on a stress-resultant/cross-sectional strains hardening plastic model, instead of enriching the model´s kinematics and related material law. One can employ weakly coupled multiscale modelling to generate constitutive relationships among the different strain and stress in a pre-processing stage. Information about plasticity, loss of geometrical stiffness and local buckling are passed to the macro-scale rod model without increasing the amount of global degrees-of-freedom. Incremental steps of the numerical solution are solved with the split operator, whereby local variables are solved in an element-wise fashion and thus not introduced in the global system. Quadratic convergence of the overall solution procedure is achieved. The coupling among geometrical and hardening effects limits the load bearing capacity of the structural members and determinates the failure load.

1 INTRODUCTION

In the current work, a first attempt for an alternative framework to 3D rod modelling is proposed and explored: a geometrically exact thin-walled beam formulation contemplating torsional warping degree of freedom, and stress-resultant-based plasticity. The plasticity parameters are analogous to the generalized strain measures of the plastic counterpart, with yield criteria based on stress resultants. It is a direct extension to the 3D case of ideas proposed by [4], which in turn were generalized for 2D finite strain Reissner rods in [2], [3].

Thin-walled elements are especially prone to instabilities, that arise from the loss of stiffness due to geometrical effects. For such structures, it is usual to have buckling modes that couples normal forces, bending, and twisting. On top of that, when inelastic constitutive equations are considered, such effects must be more carefully evaluated, since coupling material and geometrical instabilities might lead to a more complex structural behavior, which resembles, from a beam-component perspective, a failure-like generalized stress-strain curve.

Formulations that consider 3D finite strains with plasticity usually relies on solving local problems under complete 3D solid mechanics approaches (such as in [5]), which incurs into higher computational cost. Up to now, discussions about lower order models are carried either on 2D problems or in geometrically inexact theories with constraints (see [2], [6], [7], [8], [9], [10]). In plate and shell theories, the formulation of yield resultants is more direct, since there is no "master" cross-section to be accounted for: it can be dealt as a rectangular section with unitary width (see e.g. [11]). The plasticity parameters needed for simulation (namely hardening modulus, yield and ultimate resultants) are obtained by using micro-scale models with robust shell finite elements at a pre-process stage. This prevents the need for refined models at runtime, increasing workflow speed. Also, the initial micro-scale step might be reused in future simulations, given that its output can be interpreted as properties of a given cross-section.

The current work is written in a general way, allowing for an arbitrary choice of stress-resultant based yield functions, elastic and hardening constitutive equations, albeit only a simple case will be displayed here for the sake of a concise illustration. The proposed formulation can be freely tailored for specific design and research needs.

One should keep in mind that the present manuscript is a work in progress, and the current results are only partial.

Throughout the text, the notation is as follows: Greek and Latin italic lowercase letters are scalar quantities, bold Greek and Latin italic lowercase represent vectors and bold Greek and Latin italic uppercase denote second order tensors in three-dimensional Euclidean space. Summation convention over repeated indices is adopted (Einstein's notation), with Greek letter indices ranging from 1 to 2 and Latin indices from 1 to 3.

2 ROD MODEL KINEMATICS AND EQUILIBRIUM

The basic kinematical description is taken from some of the authors' previous work [1], [12], which is itself the product of decades-long research from other researchers from the same group [13], [14], [15], [16], [17], [18], [19], as well as others around the world [5], [20], [21], [22], [23], [24], [25]. The most comprehensive of the aforementioned model features a thin-walled beam that has 7 degrees of freedom (DOFs) per node, 6 for rigid body motion, and one additional one for the torsional warping.

Taking the mentioned model as starting point, one has a straight reference configuration,

taken as the same as the initial one, which can be described by the vector field

$$\boldsymbol{\xi} = \boldsymbol{\zeta} + \boldsymbol{a}^r \tag{1}$$

where $\boldsymbol{a}^r = \xi_\alpha \boldsymbol{e}_\alpha^r$ is a director vector, $\boldsymbol{\zeta} = \zeta \boldsymbol{e}_3^r$ is the axial coordinate and $\{\boldsymbol{e}_1^r, \boldsymbol{e}_2^r, \boldsymbol{e}_3^r\}$ is an orthonormal reference basis ($\{\boldsymbol{e}_1^r, \boldsymbol{e}_2^r\}$ defines the cross-sectional plane and $\boldsymbol{e}_3^r$ the rod's axis). The current configuration is given by

$$\boldsymbol{x} = \boldsymbol{z} + \boldsymbol{Q}\boldsymbol{a}^r + \boldsymbol{w} \tag{2}$$

where $\boldsymbol{z} = \boldsymbol{\zeta} + \boldsymbol{u}$ is the current position of the axis, $\boldsymbol{a} = \boldsymbol{Q}\boldsymbol{a}^r$ is the current director vector, $\boldsymbol{Q}$ is a rotation tensor, parametrized in the form of the Euler-Rodrigues parametrization (see [13], [26]) and $w = p\psi \boldsymbol{e}_3$ is the warping displacement, in which ψ is a warping function and p is the associated warping intensity. In the original formulation, $\boldsymbol{d} = [\boldsymbol{u}, \boldsymbol{\theta}, p]^T$ comprised the 7 DOFs per node of the model.

The back-rotated total deformation gradient $(\boldsymbol{F}^r = \boldsymbol{Q}^T\boldsymbol{F})$ can be decomposed multiplicatively into elastic and hardening deformation parts. Assuming that the rod strains (as defined in [1]) could be split additively as $\boldsymbol{\varepsilon}^r = \boldsymbol{\varepsilon}^{re} + \boldsymbol{\varepsilon}^{rp}$, assuming that $\boldsymbol{\varepsilon}^{rp} = \left[\overline{\boldsymbol{\eta}}_p^r \;\; \overline{\boldsymbol{\kappa}}_p^r \;\; 0 \;\; p_p'\right]^T$, one can write

$$\boldsymbol{F}^r = \boldsymbol{F}^{re}\boldsymbol{F}^{rp}, \tag{3}$$

with

$$\boldsymbol{F}^{re} = \boldsymbol{I} + \boldsymbol{\eta}^{re} \otimes \boldsymbol{e}_3^r + (\boldsymbol{\kappa}^{re} \times \boldsymbol{y}^r) \otimes \boldsymbol{e}_3^r + p\psi_{,\alpha}\boldsymbol{e}_3^r \otimes \boldsymbol{e}_\alpha^r + p'^e\psi\boldsymbol{e}_3^r \otimes \boldsymbol{e}_3^r \tag{4}$$

Using the definitions above, one can readily impose the equilibrium by means of the virtual work theorem. Integrating the stresses along the cross-sectional area, one can write the equilibrium in terms of the cross-sectional stress resultants. This procedure yields an expression with the exact same format as in the previous work

$$\delta W = \delta W_{int} - \delta W_{ext} = 0, \forall \delta \boldsymbol{d}. \tag{5}$$

with

$$\delta W_{int} = \int_{\Omega^r} [\boldsymbol{\sigma}^r \cdot \delta \boldsymbol{\varepsilon}^r] d\zeta^r \tag{6}$$

and

$$\delta W_{ext} = \int_{\Omega^r} \widehat{\boldsymbol{q}} \cdot \delta \boldsymbol{d} d\zeta^r, \tag{7}$$

With the resultants $\widehat{\boldsymbol{q}}$ of the external surface tractions and volume body forces $(\widehat{\boldsymbol{t}}, \widehat{\boldsymbol{b}})$ and

$$\boldsymbol{\sigma}^r = \int_{A^r} \begin{bmatrix} \boldsymbol{\tau}_3^r \\ \boldsymbol{y}^r \times \boldsymbol{\tau}_3^r \\ \psi_{,\alpha}\boldsymbol{\tau}_\alpha^r \cdot \boldsymbol{e}_3^r + \psi\,(\boldsymbol{\kappa}^r \times \boldsymbol{e}_3^r) \cdot \boldsymbol{\tau}_3^r \\ \psi\boldsymbol{\tau}_3^r \cdot \boldsymbol{e}_3^r \end{bmatrix} dA^r = \begin{bmatrix} \boldsymbol{n}^r \\ \boldsymbol{m}^r \\ Q \\ B \end{bmatrix}, \tag{8}$$

where $\boldsymbol{\tau}_i^r$ are the column-vectors of the back-rotated first Piola-Kirchoff stress tensor, evaluated using the elastic strains $\boldsymbol{\varepsilon}^{re}$.

Equation (5) is solved numerically through a standard FEM approach and a split step algorithm, in which, at the local phase, plasticity conditions are met (see section 4), and a consistent elastoplastic tangent stiffness $\widehat{\boldsymbol{K}}$ is obtained.

3 CONSTITUTIVE EQUATIONS

One should define constitutive equations covering elastic and plastic phases of the proposed formulation. One can for example, assume that elastic and hardening potentials are independent. For hardening, it will be assumed that there are internal parameters that are generalized strain-like variables grouped into vector $\boldsymbol{\xi}_h$. Thus, one gets

$$\Psi(\boldsymbol{\varepsilon}^{re}, \boldsymbol{\xi}_h) = \bar{\Psi}^e(\boldsymbol{\varepsilon}^{re}) + \bar{\Psi}^h(\boldsymbol{\xi}_h) \tag{9}$$

At this point, any choice can be made for the elastic potential. One can refer to [1] to see the expressions and details about the implementations of linear elastic, exact Saint-Venant and Simo-Ciarlet material in the context of the proposed rod element, for example.

For hardening, it will be assumed, for the sake of simplicity, linear relationship. Thus, one gets

$$\Psi^h(\bar{\boldsymbol{\xi}}_h) = \frac{1}{2}\boldsymbol{\xi}_h \cdot \boldsymbol{K}_h \boldsymbol{\xi}_h, \tag{10}$$

It is convenient to define now the hardening stress where $\frac{\partial \Psi^h}{\partial \xi_h} \coloneqq -\boldsymbol{q}_h$.

In the current work, $\boldsymbol{K}_h$ wil be taken as diagonal, and the procedure to obtain the actual values are described on section 4.

4 PLASTIC DISSIPATION AND RETURN ALGORITHM

The plastic update algorithm is based on consistent thermodynamic definitions. The total plastic dissipation is given by the difference of the total internal power to the rate of total free energ. Assuming that the elastic process is non-dissipative, one gets

$$\dot{D}^p = \boldsymbol{\sigma}^r \cdot \dot{\boldsymbol{\varepsilon}}^r - \dot{\Psi}. \tag{11}$$

In order to get the plastic state in a given moment in time, one should respect the Principle of Maximum Dissipation and the plastic admissibility yield, which will define the plastic evolution equations. This statement can be formulated as constrained optimization problem, and transformed into an unconstrained optimization problem through the minimization of the Lagrangian

$$\min\left[\bar{L}_p(\boldsymbol{\sigma}^r, \boldsymbol{q}_h, \dot{\boldsymbol{\gamma}})\right] = \min\left[-\dot{D}^p + \dot{\boldsymbol{\gamma}} \cdot \boldsymbol{\phi}(\boldsymbol{\sigma}^r, \boldsymbol{q}_h)\right] \tag{12}$$

with the additional Karasch-Kuhn-Tucker (KKT) optimality conditions $\dot{\gamma}_i \geq 0$; $\dot{\gamma}_i \phi_i = 0$; $\dot{\gamma}_i \phi_i = 0$, $\phi_i \leq 0$, where $\boldsymbol{\phi}(\boldsymbol{\sigma}^r, \boldsymbol{q}_h)$ is the set of yield functions. Equation (12) can be numerically solved for pseudo-time steps using the backward Euler algorithm and, in the case of non-linear elasticity or plasticity, iterative procedures shall be employed. The reader should consult consolidated literature about this process, such as [8], [11], [27].

The proposed model has no restrictions in the type of yield function to be considered. In the spirit of the low-order rod model, one should propose simple expressions directly in terms of the stress resultants. Having qualitative information about the specific engineering problem at hand, one can perform prior studies on expected failure modes, and handcraft a set of yield functions that represents the phenomenon accurately. For the sake of illustration, two simple alternatives of yield surfaces that accounts for simultaneous stress resultants are proposed.

4.1 Independent stress resultant yield function

The most basic approach is to assume that the yield function that is associated to each generalized stress resultant is independent of each other. This can be somewhat realistic in problems that are dominated by a single stress resultant (e.g simple tension, simple bending, simple shear, etc), or in failure modes that only mobilizes one degree of freedom (e.g. plastic hinges). For hardening, defining

$$s_i := \frac{|\sigma_i^r|}{\sigma_i^y - q_{h,i}}, \tag{13}$$

where σ_i^y is the initial yield stress related to a particular stress resultant. One can write the following set of yield functions $\boldsymbol{\phi}^{(1)}$

$$\phi_i^{(1)} = s_i - 1 \leq 0. \tag{14}$$

Albeit simple, this approach leads to no interaction between stress resultants during the local calculations, and in the general case is unrealistic and against safety. Also, it generates a multi-criteria approach, which must be treated with caution during numerical solution.

4.2 Simple interaction formula

Another possible simple choice would be simplified interaction formulas. This approach is a trivial choice in cases in which the load bearing capacity of members are not known for generic loadings, but can be simply determined for specific cases, usually for pure stress resultants configurations. It can be formalized as

$$\phi^{(2)} = \sum s_i^{\alpha_i} - 1 \leq 0, \tag{15}$$

where the exponents $1 \leq \alpha_i \leq 2$ can be modified to better fit the analysed member.

Expressions of this kind can be found in technical standards such as [28] and [29]. It relies on the idea that for usual isotropic members, the admissible region generated by this criterion with α_i close to 1 is a lower bound of its load bearing capacity, and thus the design is safe.

This approach leads to a yield surface that accounts for the influence of multiple stress resultants and is a single-criteria surface, which is computationally advantageous. Note that the presence of the absolute value of the stress resultants in s_i makes this function $\mathcal{C}_0$, but not $\mathcal{C}_1$, continuous, and numerical treatment must be done with care. In the present work, $\alpha_i = 2$ will be assumed, so that (15) is always continuous.

5 MULTISCALE MODELING FOR PARAMETER INFERING

The central idea of this work is to have a rod formulation that is completely based on stress resultants, avoiding plasticity computations in a microscale level at every sub-step of the global solution – instead, the microscale computations are done in a pre-processing phase with higher order models. The philosophy for the plastic parameters inference process follows [8]: one should use a hierarchically higher order model (such as a shell or 3D-solid model) capable of performing finite strain and plasticity analysis, analyze a representative segment of the structure (i.e., a piece that corresponds the longest beam element of a given cross-section) and extract from the analysis mechanically relevant data. This procedure can be regarded as a weakly coupled multiscale technique. Henceforth, the higher-level local model will be

referred to as the *micro-scale*, whilst the global rod model as the *macro-scale.* Typically, thin-walled beam members will present a hardening behavior as long as any cross-section is not completely plastic. The final failure pattern is triggered with local buckling or when the cross-section becomes completely plastic. Even though it is possible to compute the ultimate load for the case when total cross-section is in the plastic regime, closed-form expressions are not readily available to account for the coupling of geometrical and material nonlinearities combining the effects of plasticity and local buckling.

As in the aforementioned reference, one possible criterion would be to match plastic work that occurs in hardening. In order to do so, one should be able to characterize both the end of the elastic, hardening regime. Typically, one can define:

- End of elastic regime: yielding of the first material fibers
- End of hardening regime: reaching maximum stress resultant bearing capacity

It should be noted that in the present the problem has 8 stress resultants of interest, as opposed to 2 in the above mentioned previous work.

6 NUMERIC EXAMPLE

The proposed example is a study on the lateral buckling of an I-section clamped beam under transversal loading. Complete characterization is found in Figure 1. At the material level, it is assumed a bilinear elastoplastic behavior with Von-Mises yield function, with Young's modulus $E = 200GPa$, Poisson coefficient $\nu = 0.25$, the reference initial yield stress $\sigma_y = 250MPa$, and hardening modulus $K = E/10$.

It is of interest to investigate how the simultaneous presence of hardening and geometric instability impacts the load bearing capacity of this structure. Although seemingly trivial, this problem features a fully tridimensional behavior, with non-zero components for all stress-resultants and kinematical quantities after buckling. It is also relevant to explore the impact of the choice of different yield functions at the rod-element level. Benchmark is done with a reference full-scale shell model.

In order to use the proposed multiscale approach, a micro-scale shell mesh was created for a beam section with length $l = 24\ cm$, equivalent to the largest beam element used in the discretization of the example. Calculations of the reference micro-scale were carried using Ansys Mechanical [30]. 21440 quadrilateral 9-noded elements were employed. In Figure 2, it is depicted the ultimate state for some of the load configurations from Table 1.

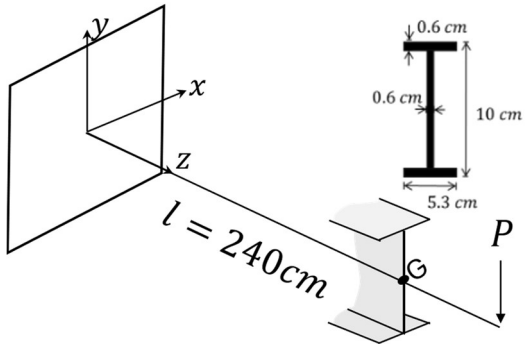

Figure 1: Example definition.

Table 1: Equivalent properties for I-section.

(Units in [cm], [kN])	Yield str.	Ultimate str.	Plastic work at ultimate state	Equivalent hardening modulus
Pure tension(1)	301.8	590	147	20930
Pure compression	301.8	3517	14636	10069
Pure shear 1	92.9	8907	335866	2834
Pure shear 2	80.1	8448	208198	4113
Torsion ($p = 0$ at both ends)	100.3	3350	10344	13005
Pure bending moment 1	1041	10777	5652	244289
Pure bending 2	198	1384	1008	22337
Pure bi-moment	673	21603	17777	315041

(1) since no ultimate strength is detected for the micro-scale, under pure tension, an arbitrary value of $\sigma_u = 500\ MPa$ is used to determine the point in which the plastic work is calculated under tension.

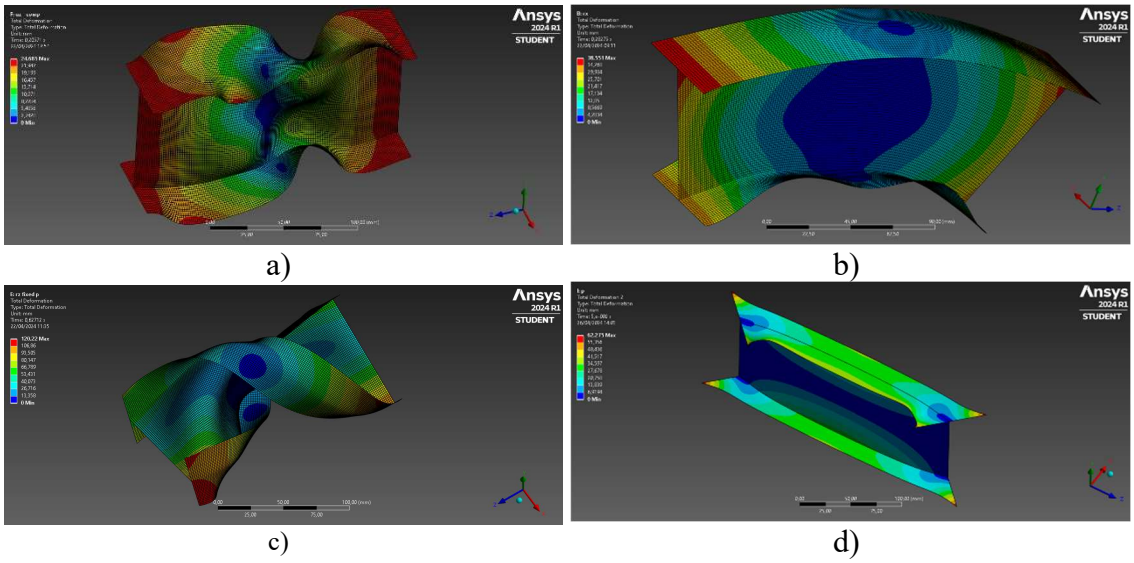

Figure 2: Ultimate load configuration for a) pure compression, b) pure bending around max. inertia axis, c) torsion without end warping; d) pure bi-moment.

Now, the values obtained in Table 1 are introduced in the rod model with proposed formulation. A mesh with 10 elements with linear interpolation is proposed. Usual Crisfield cylindrical arc-length method is employed to evaluate the equilibrium path. In Figure 3, the tip displacement is depicted for the reference (shell) and rod models with elastic and elastoplastic constitutive equations, with the two proposed stress resultant-based yield functions. For both shell and rod models, a small load perturbation is imposed at the free tip, so that bifurcation is transposed.

From Figure 3, it is clear that the yield function accounting separately for each stress resultant is not sufficient to adequately describe the failure load. However, once the rather simple interaction formula is employed, the model is capable of a much more accurate prevision

of the load bearing capacity of this structural member (characterized by the first instability see Table 2). Moreover, both elastoplastic rod models were able to preview the displacement field quite satisfactorily, even for a case in which all stress resultants were present under severe non-linear regime, due to buckling. Note that globally, this behavior resembles *softening*.

It should be noted that the presence of plastic flow equations featuring many stress resultants, and the non-smooth nature of the transition from elastic to plastic regime (and even inside different plastic steps), besides the greatly non-linear behavior from geometric effects are obstacles for the advance of the path following algorithms. In these cases, the arc-length method eventually fails at some point.

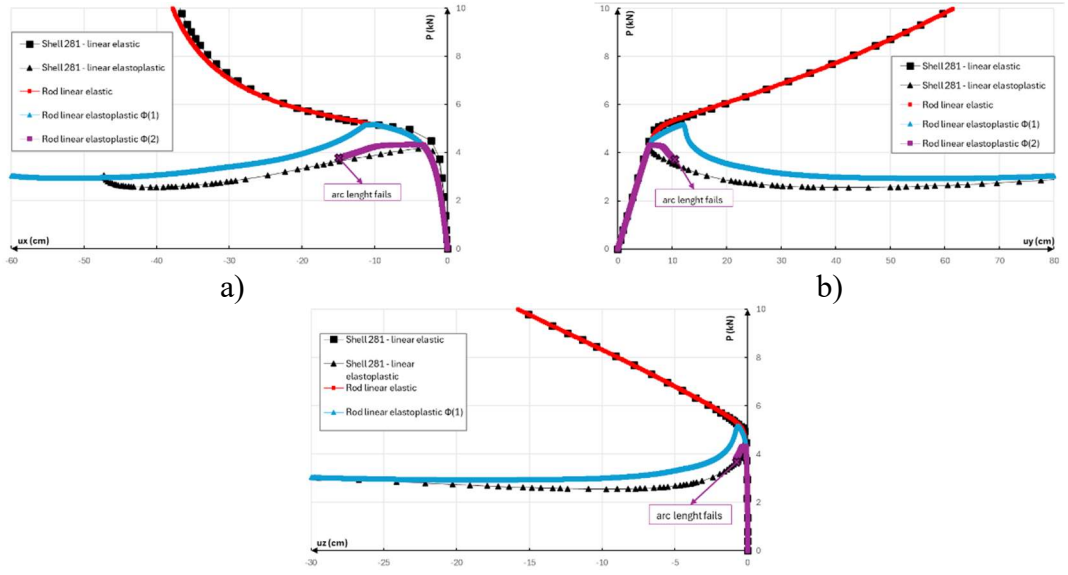

Figure 3: Equilibrium path for a) lateral displacement; b) vertical displacement; c) axial displacement.

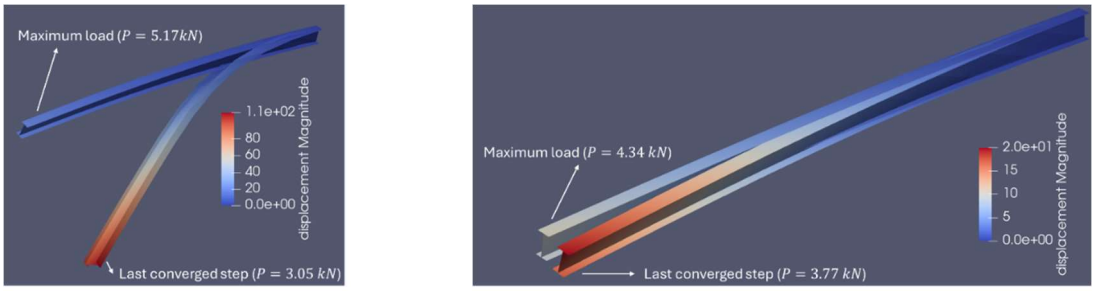

Figure 4: Deformed configuration for maximum load and last converged step for a) yield function from eq. (14); b) yield function from eq (15).

Table 2: Ultimate load for elastoplastic models, deviation from reference shell model.

	Shell	Rod $\phi^{(1)}$	Rod $\phi^{(2)}$
P (kN)	4.17	5.17 (+24%)	4.34 (+4%)

7 CONCLUSIONS

In summary, the present work performs:

- Proposition of a general description of 3D geometrically exact rod model, accounting for torsion warping and stress-resultant based hardening plasticity;
- Modular description, allowing for direct adaptation for different yield criteria, depending on the engineering problem of interest;
- Evidence of the importance of path following algorithms for non-smooth transitions in the plastic regime;
- Simple benchmark for a common steel member that is used in real-life frame structures.

ACKNOWLEDGEMENTS

This work was supported by FAPESP (Sao Paulo State Research Foundation), Brazil, under the grants 2023/16272-1 and 2022/15644-0, and CNPq (Conselho Nacional de Desenvolvimento Científico e Tecnológico), Brazil, under the grants 313046/2021-2 and 308142/2018-7, as well as by ANR (Agence Nationale Recherche) in France under the grant ANR-20-CE46-0012-01 and IUF (Institut Universitaire France) under grant 1479. The opinions, hypotheses, conclusions and recommendations expressed herein are the sole responsibility of the authors and do not necessarily reflect the funding agencies visions. Screenshots of shell models are used courtesy of ANSYS, Inc.

REFERENCES

[1] M. P. Kassab, E. M. B. Campello, and P. M. Pimenta, “Advances on kinematically exact rod models for thin-walled open-section members: Consistent warping function and nonlinear constitutive equation,” *Comput Methods Appl Mech Eng*, vol. 407, p. 115933, Mar. 2023, doi: 10.1016/j.cma.2023.115933.

[2] I. Imamovic, A. Ibrahimbegovic, and E. Mesic, “Nonlinear kinematics Reissner’s beam with combined hardening/softening elastoplasticity,” *Comput Struct*, vol. 189, pp. 12–20, Sep. 2017, doi: 10.1016/j.compstruc.2017.04.011.

[3] V. Tojaga, T. C. Gasser, A. Kulachenko, S. Östlund, and A. Ibrahimbegovic, “Geometrically exact beam theory with embedded strong discontinuities for the modeling of failure in structures. Part I: Formulation and finite element implementation,” *Comput Methods Appl Mech Eng*, vol. 410, p. 116013, May 2023, doi: 10.1016/j.cma.2023.116013.

[4] A. Ibrahimbegovic, R. Mejia-Nava, and S. Ljukovac, “Reduced model for fracture of geometrically exact planar beam: Non-local variational formulation, ED-FEM approximation and operator split solution,” *Int J Numer Methods Eng*, vol. 125, no. 1, Jan. 2024, doi: 10.1002/nme.7369.

[5] E. Hajdo, A. Ibrahimbegovic, and S. Dolarevic1, “Buckling analysis of complex structures with refined model built of frame and shell finite elements,” *Coupled Systems Mechanics*, vol. 9, no. 1, pp. 29–46, Feb. 2020, doi: 10.12989/csm.2020.9.1.029.

[6] I. Imamovic, A. Ibrahimbegovic, and E. Mesic, "Coupled testing-modeling approach to ultimate state computation of steel structure with connections for statics and dynamics," *Coupled Systems Mechanics*, vol. 7, no. 5, pp. 555–581, Oct. 2018, doi: 10.12989/csm.2018.7.5.555.

[7] J. C. Simo, K. D. Hjelmstad, and R. L. Taylor, "Numerical formulations of elasto-viscoplastic response of beams accounting for the effect of shear," *Comput Methods Appl Mech Eng*, vol. 42, no. 3, pp. 301–330, Mar. 1984, doi: 10.1016/0045-7825(84)90011-2.

[8] J. Dujc, B. Brank, and A. Ibrahimbegovic, "Multi-scale computational model for failure analysis of metal frames that includes softening and local buckling," *Comput Methods Appl Mech Eng*, vol. 199, no. 21–22, pp. 1371–1385, Apr. 2010, doi: 10.1016/j.cma.2009.09.003.

[9] D. Ehrlich and F. Armero, "Finite element methods for the analysis of softening plastic hinges in beams and frames," *Comput Mech*, vol. 35, no. 4, pp. 237–264, Mar. 2005, doi: 10.1007/s00466-004-0575-z.

[10] A. Saritas, "Stress resultants plasticity with general closest point projection," *Mech Res Commun*, vol. 38, no. 2, pp. 126–130, Mar. 2011, doi: 10.1016/j.mechrescom.2011.01.010.

[11] A. Ibrahimbegović and F. Frey, "An efficient implementation of stress resultant plasticity in analysis of Reissner-Mindlin plates," *Int J Numer Methods Eng*, vol. 36, no. 2, pp. 303–320, Jan. 1993, doi: 10.1002/nme.1620360209.

[12] E. M. B. Campello and L. B. Lago, "Effect of higher order constitutive terms on the elastic buckling of thin-walled rods," *Thin-Walled Structures*, vol. 77, pp. 8–16, Apr. 2014, doi: 10.1016/j.tws.2013.11.001.

[13] P. M. Pimenta and T. Yojo, "Geometrically Exact Analysis of Spatial Frames," *Appl Mech Rev*, vol. 46, no. 11S, pp. S118–S128, Nov. 1993, doi: 10.1115/1.3122626.

[14] P. M. Pimenta, "Constitutive second order effects on ageometrically exact finite strain rod model," in *Recent developments in solid mechanics*, Rio de Janeiro: LNCC, 1996, pp. 79–85.

[15] P. M. Pimenta and E. M. B. Campello, "Geometrically nonlinear analysis of thin-walled space frames," Proceedings of the II ECCM (European Conference on Computational Mechanics), 2001, p. 20.

[16] P. M. Pimenta and E. M. B. Campello, "A fully nonlinear multi-parameter rod model incorporating general cross-sectional in-plane changes and out-of-plane warping," *Latin American Journal of Solids and Structures*, vol. 1, no. 1, pp. 119–140, 2003.

[17] E. R. Dasambiagio, P. M. Pimenta, and E. M. B. Campello, "A finite strain rod model that incorporates general cross section deformation and its implementation by the Finite Element Method," in *Mechanics of Solids in Brazil 2009*, 1st ed., vol. 1, H. S. da Costa Mattos and M. Alves, Eds., Rio de Janeiro: Brazilian Society of Mechanical Sciences and Engineering, 2009, pp. 145–168.

[18] C. Costa e Silva, S. F. Maassen, P. M. Pimenta, and J. Schröder, "On the simultaneous use of simple geometrically exact shear-rigid rod and shell finite elements," *Comput Mech*, vol. 67, no. 3, pp. 867–881, Mar. 2021, doi: 10.1007/s00466-020-01967-2.

[19] C. da Costa e Silva, S. F. Maassen, P. M. Pimenta, and J. Schröder, "A simple finite element for the geometrically exact analysis of Bernoulli–Euler rods," *Comput Mech*, vol. 65, no. 4, pp. 905–923, Apr. 2020, doi: 10.1007/s00466-019-01800-5.

[20] J. C. Simo, "A finite strain beam formulation. The three-dimensional dynamic problem. Part I," *Comput Methods Appl Mech Eng*, vol. 49, no. 1, pp. 55–70, May 1985, doi: 10.1016/0045-7825(85)90050-7.

[21] J. C. Simo and L. Vu-Quoc, "A three-dimensional finite-strain rod model. part II: Computational aspects," *Comput Methods Appl Mech Eng*, vol. 58, no. 1, pp. 79–116, Oct. 1986, doi: 10.1016/0045-7825(86)90079-4.

[22] J. C. Simo and L. Vu-Quoc, "A Geometrically-exact rod model incorporating shear and torsion-warping deformation," *Int J Solids Struct*, vol. 27, no. 3, pp. 371–393, 1991, doi: 10.1016/0020-7683(91)90089-X.

[23] A. Ibrahimbegović, H. Shakourzadeh, J.-L. Batoz, M. AI Mikdad, and Y.-Q. Guo, "On the role of geometrically exact and second-order theories in buckling and post-buckling analysis of three-dimensional beam structures," *Comput Struct*, vol. 61, no. 6, pp. 1101–1114, Dec. 1996, doi: 10.1016/0045-7949(96)00181-2.

[24] A. Ibrahimbegović, F. Frey, and I. Kožar, "Computational aspects of vector-like parametrization of three-dimensional finite rotations," *Int J Numer Methods Eng*, vol. 38, no. 21, pp. 3653–3673, Nov. 1995, doi: 10.1002/nme.1620382107.

[25] A. Ibrahimbegović and F. Frey, "Finite element analysis of linear and non-linear planar deformations of elastic initially curved beams," *Int J Numer Methods Eng*, vol. 36, no. 19, pp. 3239–3258, Oct. 1993, doi: 10.1002/nme.1620361903.

[26] A. Ibrahimbegovic, "On the choice of finite rotation parameters," *Comput Methods Appl Mech Eng*, vol. 149, no. 1–4, pp. 49–71, Oct. 1997, doi: 10.1016/S0045-7825(97)00059-5.

[27] A. Ibrahimbegovic, *Nonlinear Solid Mechanics*, vol. 160. Dordrecht: Springer Netherlands, 2009. doi: 10.1007/978-90-481-2331-5.

[28] ASSOCIAÇÃO BRASILEIRA DE NORMAS TÉCNICAS, *ABNT NBR 8800:2008: Projeto de estruturas de aço e de estruturas mistas de aço e concreto de edifícios*, ABNT. Rio de Janeiro, 2008.

[29] British Standards Institution, *EN 1933-1-1. Eurocode 3: Design of steel structures - Part 1-1: General rules and rules for buildings* , BSI. London, 2010.

[30] ANSYS Inc, "Ansys Mechanical User's Guide." ANSYS Inc, Canonsburg, PA, USA, 2013.